HHS Public Access

Author manuscript

Biochim Biophys Acta. Author manuscript; available in PMC 2017 October 01.

Published in final edited form as:

Biochim Biophys Acta. 2016 October ; 1860(10): 2148–2156. doi:10.1016/j.bbagen.2016.05.027.

Limited Versus Total Epithelial Debridement Ocular Surface Injury: Live Fluorescence Imaging of Hemangiogenesis and Lymphangiogenesis in Prox1-GFP/Flk1::myr-mCherry Mice

Jin-Hong Chang, PhD[1,*], **Ilham Putra, MD**[1], **Yu-hui Huang, MS**[1], **Michael Chang, BS**[1], **Kyuyeon Han, PhD**[1], **Wei Zhong, MD**[1], **Xinbo Gao, MD, PhD**[1], **Shuangyong Wang, MD, PhD**[1], **Jennifer Dugas-Ford, PhD**[1], **Tara Nguyen, BS**, **Young-Kwon Hong, PhD**[2], and **Dimitri T. Azar, MD, MBA**[1,*]

[1]Department of Ophthalmology and Visual Sciences, Illinois Eye and Ear Infirmary, College of medicine, University of Illinois at Chicago, Chicago, Illinois

[2]Department of Surgery, Norris Comprehensive Cancer Center, Keck School of Medicine, University of Southern California, Los Angeles, CA, USA

Abstract

Background—Immunohistochemical staining experiments have shown that both hemangiogenesis and lymphangiogenesis occur following severe corneal and conjunctival injury and that the neovascularization of the cornea often has severe visual consequences. To better understand how hemangiogenesis and lymphangiogenesis are induced by different degrees of ocular injury, we investigated patterns of injury-induced corneal neovascularization in live *Prox1-GFP/Flk1::myr-mCherry* mice, in which blood and lymphatic vessels can be imaged simultaneously *in vivo*.

Methods—The eyes of Prox1-GFP/Flk1::myr-mCherry mice were injured according to four models based on epithelial debridement of the: A) central cornea (a 1.5-mm-diameter circle of tissue over the corneal apex), B) total cornea, C) bulbar conjunctiva, and D) cornea+bulbar conjunctiva. Corneal blood and lymphatic vessels were imaged on days 0, 3, 7, and 10 post-injury, and the percentages of the cornea containing blood and lymphatic vessels were calculated.

Results—Neither central corneal nor bulbar conjunctival debridement resulted in significant vessel growth in the mouse cornea, whereas total corneal and corneal+bulbar conjunctival debridement did. On day 10 in the central cornea, total cornea, bulbar conjunctiva, and corneal +bulbar conjunctival epithelial debridement models, the percentage of the corneal surface that was occupied by blood vessels (hemangiogenesis) was 1.9±0.8%, 7.14±2.4%, 2.29±1%, and 15.05±2.14%, respectively, and the percentage of the corneal surface that was occupied by

[*]Address correspondence to Jin-Hong Chang, Ph.D. (changr@uic.edu) and Dimitri T. Azar, MD, MBA (dazar@uic.edu), Department of Ophthalmology and Visual Sciences, University of Illinois at Chicago, 1855 W. Taylor Street, Chicago, IL 60612.

Conflict of interest: The authors have no conflicts of interest to declare.

lymphatic vessels (lymphangiogenesis) was 2.45±1.51%, 4.85±0.95%, 2.95±1.27%, and 4.15±3.85%, respectively.

Conclusions—Substantial corneal debridement was required to induce corneal neovascularization in the mouse cornea, and the corneal epithelium may therefore be partially responsible for maintaining corneal avascularity.

General significance—Our study demonstrates that GFP/Flk1::myr-mCherry mice are a useful model for studying coordinated hemangiogenic and lymphangiogenic responses.

Keywords

Cornea; bulbar conjunctiva; corneal neovascularization (NV); hemangiogenesis (HA); lymphangiogenesis (LA); *in vivo* imaging

1. Introduction

Decades of research have revealed that hemangiogenesis (HA) plays many important roles in normal development as well as in disease progression [1–3]. In comparison, the importance and mechanisms of lymphangiogenesis (LA) remain poorly understood, primarily because lymphatic vessels are not perfused with blood cells and thus cannot be visually observed [4]. Still, over the past 20 years, molecular markers for lymphatic vessels have been identified and characterized using immunohistochemical staining in LA-related research. Markers of lymphatic endothelial cells (LECs), such as lymphatic vessel endothelial hyaluronan receptor-1 (LYVE-1) [5], PROX-1 [6, 7], podoplanin [8], and vascular endothelial growth factor receptor 3 (VEGFR3)[9], have been used to show that while HA and LA are often induced independently, under certain experimental conditions, they can be concomitantly induced [7, 10–12].

The adult cornea is necessarily avascular to facilitate clear vision, and this characteristic makes the cornea an exceptionally good model for *in vivo* monitoring and for characterizing injury-induced HA and LA. While a healthy cornea must not contain blood vessels, it is encircled by vessels at the limbus. Neovascularization (NV) describes the formation of new vascular structures in areas that were previously avascular. Corneal neovascularization is a sight-threatening condition that is usually associated with inflammatory, infectious disorders of the ocular surface and loss of immune privilege. After injury, corneal NV arises from existing vascular networks and is characterized by the ingrowth of visible blood and lymphatic vessels into the cornea from the limbus. Harvested corneas can be immunohistochemically stained to explore how HA and LA are induced in the cornea in response to various stimuli. Both HA and LA are stimulated by the release of vascular endothelial growth factors (VEGFs) from inflammatory cells, which are induced to invade the cornea in response to hypoxic or inflammatory conditions [13–15]. However, LA and HA can also occur independent of VEGF following the delivery of a low dose of fibroblast growth factor (FGF)-2 within the cornea (12.5 ng/pellet) [16]. Using an *in vivo* model to study HA and LA, Cao et al. [17] showed that implanting VEGF-A, VEGF-C, or basic FGF (bFGF) into the mouse cornea elicited a robust lymphangiogenic response. We developed a different *in vivo* model that permits the study of both LA and HA that does not require the

sacrifice of the animals to visualize blood and lymphatic vessels (for postmortem staining). Using our *prox1-GFP/Flk1::myr-mCherry* transgenic mice, LA and HA can be simultaneously imaged *in vivo*. We previously demonstrated the feasibility of using these mice to evaluate corneal LA and HA [7].

The roles of the limbus and the bulbar conjunctiva in corneal neovascularization (NV) are not well understood, and studies have reported conflicting results regarding whether the limbus acts as a barrier to infiltrating vessels [18–21]. The limbus contains many specialized cell types, including multipotent stem cells that are required for repopulating the cornea following injury [22–24]. Within the limbus is a dense vascular network of blood and lymphatic vessels. Pathologies such as limbal stem cell deficiency and conjunctival epithelial injury can result in corneal inflammation and NV [25]. Minor injuries to the cornea rarely result in the invasion of blood and lymphatic vessels from the adjacent, heavily vascularized limbus. In contrast, an extensive corneal injury, especially when combined with conjunctival epithelial injury, may require LA and HA to repair the damaged tissue.

Here, we present an *in vivo,* longitudinal, imaging-based comparative analysis of HA and LA that was induced by four models of epithelial corneal and bulbar conjunctival injury in the same live transgenic mice over time.

2. Materials and Methods

2.1 Animal Care

Male and female (6–8 weeks old) *Prox1-GFP/Flk1::myr-mCherry* mice [7] were divided into four groups (n=5 in all groups) according to the injury that was applied: central (a 1.5-mm-diameter circle of tissue at the apex of the cornea) corneal debridement (Fig. 1A), total corneal debridement (Fig. 1B)[26, 27], bulbar conjunctival debridement (Fig. 1C), and corneal+bulbar conjunctival debridement (Fig. 1D). Before surgeries and *in vivo* imaging were performed, the mice were anesthetized using an intraperitoneal injection of ketamine hydrochloride (100 mg/kg; Hospira, Inc., Lake Forest, IL) and xylazine (5 mg/kg; Lloyd Laboratories, Shenandoah, IA) and then treated with topical 1% proparacaine eye drops (Sandoz, Inc., Princeton, NJ). The eyelashes were clipped above and below the eye in preparation for both surgical procedures and *in vivo* imaging. All animals were handled in accordance with the Association for Research in Vision and Ophthalmology Statement for the Use of Animals in Ophthalmic and Vision Research.

2.2 Epithelial Debridement

A corneal rust ring remover (Alger Brush II, Latham & Phillips Ophthalmic, Grove City, OH) was used to brush-debride the epithelium of the cornea and/or the bulbar conjunctiva [28]. Following debridement, one or two drops of fluorescein dye were applied to the eye to verify the removal of the epithelium within the targeted region. The eyes were visualized under a Nikon D3X camera mounted on a Zeiss S88 microscope (Zeiss Microscopy, Oberkochen, Germany). After debridement, the eye was rinsed with saline, and an erythromycin ointment (Bausch and Lomb, Tampa, FL) was topically applied. Intramuscular

injections of 0.1 ml of 0.3 mg/ml buprenorphine (Buprenex; Reckitt Benckiser Healthcare, Hull, UK) were administered post-operation and twice on the following day to relieve pain.

2.3 Fluorescence Microscopy

NV was assessed using *in vivo* fluorescence microscopy throughout the wound healing process. *In vivo* imaging was performed in all mice using a Carl Zeiss AXIOZOOM V16 (Carl Zeiss Microscopy) prior to surgery and on post-operative days 3, 7, and 10. The mice were immobilized during microscopy using a stereotactic frame. The camera Axiocam HRm was focused onto the cornea at 30× magnification. The exposure times were 30 ms and 100 ms for GFP and mCherry detection, respectively. Z-stack images were taken from the base of the cornea to its apex, and the images were merged. Frontal and lateral views of the cornea were obtained.

2.4 Quantification of Corneal NV

The collected fluorescence images were compiled, analyzed, and quantified using Adobe Photoshop CS5 image software (Adobe Systems Inc., San Jose, CA). Within a particular image, the region of interest of the cornea was selected and considered as a total area. Visual conditions, such as brightness and contrast, were then adjusted to clearly distinguish blood and lymphatic vessels. For some areas in which blood vessels appeared blurry, extreme care was taken to properly analyze the vessel area. The percentage of the total corneal area that was occupied by blood vessels [(area of blood vessels/total cornea area) × 100] was used as a measure of corneal HA. The percentage of the total corneal area that was occupied by lymphatic vessels [(area of lymphatic vessels/total cornea area) × 100] was used as a measure of corneal LA.

2.5 Statistical Analysis

All data are expressed as the mean ± standard error of the mean (SEM). To quantify changes in corneal HA and LA, the measurements that were taken for each metric at each time point were compared to the previously obtained baseline values. Differences in the experimental data were analyzed using the Student t-test in MS Excel. In all cases, a value of $P < 0.05$ was considered statistically significant. Statistical values were calculated, and comparison graphs were generated in MS Excel.

3. Results

3.1 In Vivo Fluorescence Imaging of Injury-induced Corneal NV

When the cornea was injured within a 1.5-mm-diameter circle that was centered on the apex of the cornea, the conjunctiva was undamaged and appeared normal at all time points. In addition, no significant blood or lymphatic vessel growth from the limbus into the cornea was observed at days 7 and 10. (Fig. 2).

When the whole cornea was debrided, the conjunctiva was undamaged and appeared normal at all time points. However, HA and LA had progressed from the limbus into the cornea by post-operative day 3, and continuous progression was observed on postoperative days 7 and 10. HA extended farther into the cornea than LA (Fig. 3).

Prior to wounding, lymphatic vessels were apparent within the limbus. However, when the bulbar conjunctiva was debrided, lymphatic vessels were lost by post-operative day 3, and this loss persisted for the remainder of the study (Fig. 4). The limbal vessels did not show any significant advancement into the cornea on post-operative day 10 (Fig. 4), and HA remain unchanged throughout the protocol.

When both the corneal epithelium and the conjunctival epithelium were debrided, well-defined blood and lymphatic vasculatures were observed on post-operative day 3 (Fig. 5). By post-operative day 7, a dense network of blood vessels was observed to have invaded the cornea from the limbus, and further progression was observed on postoperative day 10 (Fig. 5). In contrast, the number of lymphatic vessels remained below the baseline value.

3.2 Quantitative Assessment of Injury-induced Corneal NV

The percentages of the areas of the cornea that were occupied by new-growth blood and lymphatic vessels were calculated for each experimental group at each time point after injury. On day 10, the percentages of the corneal surface occupied by HA were 1.9±0.8%, 7.14±2.4%, 2.29±1%, and 15.05±2.14% in the central cornea, total cornea, bulbar conjunctiva, and corneal+bulbar conjunctival epithelial debridement models, respectively (Fig. 6A), and the percentages of the corneal surface occupied by LA were 2.45±1.51%, 4.85±0.95%, 2.95±1.27%, and 4.15±3.85% in the central cornea, total cornea, bulbar conjunctiva, and corneal+bulbar conjunctival epithelial debridement models, respectively (Fig. 6B).

Figure 6C shows that a significant difference was detected between the experimental models in the percentage of HA that was observed on day 10 (central cornea, 1.9±0.8% vs. total cornea, 7.14±2.4%, $P < 0.01$; central cornea, 1.9±0.8% vs. cornea+bulbar conjunctiva, 15.05±2.14%, $P < 0.00001$; cornea, 7.14±2.4% vs. bulbar conjunctiva, 2.29±1%, $P < 0.05$; cornea, 7.14%±2.4% vs. cornea+bulbar conjunctiva, 15.05%±2.14%, $P < 0.001$; and bulbar conjunctiva, 2.29±1% vs. cornea+ conjunctiva, 15.05±2.14%, $P < 0.05$) and in the percentage of LA that was observed on day 10 (central cornea, 2.45±1.51% vs. cornea, 4.85±0.95%, $P < 0.05$).

In contrast, in the central corneal and bulbar conjunctiva, only the epithelial debridement mouse models showed no significant differences in HA and LA compared to the control mice (Fig. 6C). This finding suggests that a substantial amount of corneal debridement may be necessary to induce corneal NV. However, bulbar conjunctival debridement appears to play a significant role only when combined with total corneal debridement, because this prominent HA but no significant HA or LA was observed with conjunctival debridement only.

The quantified results shown in Figure 6 demonstrate that central corneal debridement and conjunctival debridement did not induce significant vessel growth at any time point, whereas total corneal debridement and debridement of both the cornea and the bulbar conjunctiva induced significant HA and LA by post-operative days 7 and 10 (all $P < 0.05$). In both the total corneal debridement and the corneal+bulbar conjunctival debridement groups, the observed HA was considerably more extensive than the observed LA.

Figure 7 shows that the number of endpoints of blood vessels increased gradually. A decline in the number of lymphatic vessel endpoints at day 3 was caused by the loss of lymphatic vessels during corneal+bulbar scraping. The number of blood vessel endpoints remained unaffected, as they are generally more prominent in the basement area than in the epithelium. The lengths of blood and lymphatic vessels that grew into the cornea were compared over the course of 10 days. Lymphatic vessels did not show any significant growth in terms of length by day 3 after corneal+bulbar scraping, because more time is needed for these vessels to re-grow into the cornea from the basement membrane. Beyond day 3, the length of growing lymphatic vessels increased gradually.

To illustrate how HA and LA can be visualized in tissues other than the cornea using this mouse model, we collected samples of skin and tail for confocal imaging (Figure 8). The observation of distinct blood and lymphatic vessels in these samples via confocal imaging demonstrates the potential of this platform for extending our research of HA and LA beyond the cornea. Notably, surface tissues such as skin and tail are easily accessible for inducing HA and LA using injury models and then imaging subsequent vessel growth.

4. Discussion

Using *Prox1-GFP/Flk1::myr-mCherry* mice, in which blood and lymphatic vessels are fluorescently labeled, we were able to observe the HA and LA response to injuries inflicted on the cornea and bulbar conjunctiva using epithelial debridement. Our results demonstrate that substantial corneal epithelial debridement is required to induce corneal NV because neither central corneal debridement nor bulbar conjunctival debridement induced a significant amount of growth of either vessel type. In contrast, total corneal debridement and corneal+bulbar conjunctival debridement induced prominent NV, suggesting that the corneal epithelium is critically responsible for maintaining corneal avascularity. In addition, the absence of lymphatic vessels in the corneas of eyes in which the bulbar conjunctiva was debrided suggests that lymphatic vessels are located more superficially than blood vessels within the corneal epithelium, while blood vessels reside deeper in the corneal stromal layers.

In these experiments, we used a cornea rust ring remover to selectively remove the bulbar conjunctival region in a controlled manner. Previously used methods to remove the conjunctival region have involved the use of caustic agents, but these also cause additional, unnecessary damage to the eye because it is inherently difficult to control the application of the agent. The use of a cornea rust ring remover is beneficial for studying the effects of removing the bulbar conjunctiva because this tool offers fine control and thereby prevents unnecessary damage.

A number of causal pro- and anti-angiogenic factors have been identified, including members of the VEGF family of ligands and receptors, bFGFs, and matrix metalloproteinases (MMPs) [3, 20], while anti-angiogenic factors include other members of the VEGF family in addition to angiostatin and endostatin [29]. The corneal epithelium produces both pro- and anti-angiogenic factors. The secreted forms of VEGFR-1, -2 and -3 are also produced in the corneal epithelium [30–33]. The VEGFR family is involved in both

HA and LA, depending on the receptor subtype. VEGFR-1 is anti-angiogenic, and the deletion of soluble VEGFR-1 resulted in the spontaneous invasion of blood vessels into the cornea [30]. In contrast, VEGFR2 prevents LA, and the deletion of sVEGFR2 resulted in spontaneous lymphatic vessel growth into the cornea [31]. Therefore, both of these factors are required for the maintenance of avascularity in the cornea.

Using methods allowing the simultaneous *in vivo* imaging of HA and LA in the corneas of live *Prox1-GFP/Flk1::myr-mCherry* mice, the experiments described in the present study characterize the patterns of HA and LA that were induced in response to injury by debridement in addition to the relative contributions of the corneal and conjunctival epithelia to injury-induced HA and LA. This study confirms that *GFP/Flk1::myr-mCherry* mice are a useful model for observing coordinated hemangiogenic and lymphangiogenic responses *in vivo*, and these findings can be applied in the future research aimed at developing therapies targeting HA and/or LA in the cornea.

Supplementary Material

Refer to Web version on PubMed Central for supplementary material.

Acknowledgments

This study was supported by grants from the National Institutes of Health [EY10101 (D.T.A.), EY023691, EY021886, I01 BX002386 (J.H.C), and EY01792] and an unrestricted grant from Research to Prevent Blindness, New York, NY.

Abbreviations

NV	neovascularization
HA	hemangiogenesis
LA	lymphangiogenesis
Flk	fetal liver kinase
GFP	green fluorescent protein
Prox-1	Prospero Homeobox 1
VEGF	vascular endothelial growth factor
VEGFR	vascular endothelial growth factor receptor

References

1. He Y, Karpanen T, Alitalo K. Role of lymphangiogenic factors in tumor metastasis. Biochimica et biophysica acta. 2004; 1654:3–12. [PubMed: 14984763]
2. Eklund L, Bry M, Alitalo K. Mouse models for studying angiogenesis and lymphangiogenesis in cancer. Molecular oncology. 2013; 7:259–282. [PubMed: 23522958]
3. Stacker SA, Williams SP, Karnezis T, Shayan R, Fox SB, Achen MG. Lymphangiogenesis and lymphatic vessel remodelling in cancer. Nature reviews Cancer. 2014; 14:159–172. [PubMed: 24561443]

4. Yang JF, Walia A, Huang YH, Han KY, Rosenblatt MI, Azar DT, Chang JH. Understanding Lymphangiogenesis in Knockout Models, the Cornea, and Ocular Diseases for the Development of Therapeutic Interventions. Survey of ophthalmology. 2015
5. Johnson LA, Prevo R, Clasper S, Jackson DG. Inflammation-induced uptake and degradation of the lymphatic endothelial hyaluronan receptor LYVE-1. The Journal of biological chemistry. 2007; 282:33671–33680. [PubMed: 17884820]
6. Martinez-Corral I, Ulvmar MH, Stanczuk L, Tatin F, Kizhatil K, John SW, Alitalo K, Ortega S, Makinen T. Nonvenous origin of dermal lymphatic vasculature. Circulation research. 2015; 116:1649–1654. [PubMed: 25737499]
7. Zhu J, Dugas-Ford J, Chang M, Purta P, Han KY, Hong YK, Dickinson ME, Rosenblatt MI, Chang JH, Azar DT. Simultaneous in vivo imaging of blood and lymphatic vessel growth in Prox1-GFP/Flk1::myr-mCherry mice. The FEBS journal. 2015
8. Herwig MC, Munstermann K, Klarmann-Schulz U, Schlereth SL, Heindl LM, Loeffler KU, Muller AM. Expression of the lymphatic marker podoplanin (D2–40) in human fetal eyes. Experimental eye research. 2014; 127:243–251. [PubMed: 25135789]
9. Deng Y, Zhang X, Simons M. Molecular controls of lymphatic VEGFR3 signaling. Arteriosclerosis, thrombosis, and vascular biology. 2015; 35:421–429.
10. Adams RH, Alitalo K. Molecular regulation of angiogenesis and lymphangiogenesis. Nature reviews Molecular cell biology. 2007; 8:464–478. [PubMed: 17522591]
11. Yuen D, Wu X, Kwan AC, Ledue J, Zhang H, Ecoiffier T, Pytowski B, Chen L. Live imaging of newly formed lymphatic vessels in the cornea. Cell research. 2011; 21:1745–1749. [PubMed: 22083511]
12. Truong TN, Li H, Hong YK, Chen L. Novel characterization and live imaging of Schlemm's canal expressing Prox-1. PloS one. 2014; 9:e98245. [PubMed: 24827370]
13. Lee HS, Hos D, Blanco T, Bock F, Reyes NJ, Mathew R, Cursiefen C, Dana R, Saban DR. Involvement of corneal lymphangiogenesis in a mouse model of allergic eye disease. Investigative ophthalmology & visual science. 2015; 56:3140–3148. [PubMed: 26024097]
14. Zampell JC, Yan A, Avraham T, Daluvoy S, Weitman ES, Mehrara BJ. HIF-1alpha coordinates lymphangiogenesis during wound healing and in response to inflammation. FASEB journal : official publication of the Federation of American Societies for Experimental Biology. 2012; 26:1027–1039. [PubMed: 22067482]
15. Cao R, Ji H, Feng N, Zhang Y, Yang X, Andersson P, Sun Y, Tritsaris K, Hansen AJ, Dissing S, Cao Y. Collaborative interplay between FGF-2 and VEGF-C promotes lymphangiogenesis and metastasis. Proceedings of the National Academy of Sciences of the United States of America. 2012; 109:15894–15899. [PubMed: 22967508]
16. Chang LK, Garcia-Cardena G, Farnebo F, Fannon M, Chen EJ, Butterfield C, Moses MA, Mulligan RC, Folkman J, Kaipainen A. Dose-dependent response of FGF-2 for lymphangiogenesis. Proceedings of the National Academy of Sciences of the United States of America. 2004; 101:11658–11663. [PubMed: 15289610]
17. Cao R, Lim S, Ji H, Zhang Y, Yang Y, Honek J, Hedlund EM, Cao Y. Mouse corneal lymphangiogenesis model. Nature protocols. 2011; 6:817–826. [PubMed: 21637201]
18. Chang JH, Gabison EE, Kato T, Azar DT. Corneal neovascularization. Curr Opin Ophthalmol. 2001; 12:242–249. [PubMed: 11507336]
19. Chang JH, Garg NK, Lunde E, Han KY, Jain S, Azar DT. Corneal neovascularization: an anti-VEGF therapy review. Survey of ophthalmology. 2012; 57:415–429. [PubMed: 22898649]
20. Chang JH, Huang YH, Cunningham CM, Han KY, Chang M, Seiki M, Zhou Z, Azar DT. Matrix metalloproteinase 14 modulates signal transduction and angiogenesis in the cornea. Survey of ophthalmology. 2015
21. Azar DT. Corneal angiogenic privilege: angiogenic and antiangiogenic factors in corneal avascularity, vasculogenesis, and wound healing (an American Ophthalmological Society thesis). Trans Am Ophthalmol Soc. 2006; 104:264–302. [PubMed: 17471348]
22. Stepp MA, Zieske JD, Trinkaus-Randall V, Kyne BM, Pal-Ghosh S, Tadvalkar G, Pajoohesh-Ganji A. Wounding the cornea to learn how it heals. Experimental eye research. 2014; 121:178–193. [PubMed: 24607489]

23. Ebato B, Friend J, Thoft RA. Comparison of limbal and peripheral human corneal epithelium in tissue culture. Investigative ophthalmology & visual science. 1988; 29:1533–1537. [PubMed: 3170124]
24. Tsai RJ, Sun TT, Tseng SC. Comparison of limbal and conjunctival autograft transplantation in corneal surface reconstruction in rabbits. Ophthalmology. 1990; 97:446–455. [PubMed: 1691476]
25. Pajoohesh-Ganji A, Pal-Ghosh S, Tadvalkar G, Stepp MA. Corneal goblet cells and their niche: implications for corneal stem cell deficiency. Stem Cells. 2012; 30:2032–2043. [PubMed: 22821715]
26. Pal-Ghosh S, Pajoohesh-Ganji A, Tadvalkar G, Kyne BM, Guo X, Zieske JD, Stepp MA. Topical Mitomycin-C enhances subbasal nerve regeneration and reduces erosion frequency in the debridement wounded mouse cornea. Experimental eye research. 2015
27. Pajoohesh-Ganji A, Pal-Ghosh S, Tadvalkar G, Kyne BM, Saban DR, Stepp MA. Partial denervation of sub-basal axons persists following debridement wounds to the mouse cornea. Laboratory investigation; a journal of technical methods and pathology. 2015; 95:1305–1318.
28. Gronert K, Maheshwari N, Khan N, Hassan IR, Dunn M, Laniado Schwartzman M. A role for the mouse 12/15-lipoxygenase pathway in promoting epithelial wound healing and host defense. The Journal of biological chemistry. 2005; 280:15267–15278. [PubMed: 15708862]
29. Walia A, Yang JF, Huang YH, Rosenblatt MI, Chang JH, Azar DT. Endostatin's emerging roles in angiogenesis, lymphangiogenesis, disease, and clinical applications. Biochimica et biophysica acta. 2015; 1850:2422–2438. [PubMed: 26367079]
30. Ambati BK, Nozaki M, Singh N, Takeda A, Jani PD, Suthar T, Albuquerque RJ, Richter E, Sakurai E, Newcomb MT, Kleinman ME, Caldwell RB, Lin Q, Ogura Y, Orecchia A, Samuelson DA, Agnew DW, St Leger J, Green WR, Mahasreshti PJ, Curiel DT, Kwan D, Marsh H, Ikeda S, Leiper LJ, Collinson JM, Bogdanovich S, Khurana TS, Shibuya M, Baldwin ME, Ferrara N, Gerber HP, De Falco S, Witta J, Baffi JZ, Raisler BJ, Ambati J. Corneal avascularity is due to soluble VEGF receptor-1. Nature. 2006; 443:993–997. [PubMed: 17051153]
31. Albuquerque RJ, Hayashi T, Cho WG, Kleinman ME, Dridi S, Takeda A, Baffi JZ, Yamada K, Kaneko H, Green MG, Chappell J, Wilting J, Weich HA, Yamagami S, Amano S, Mizuki N, Alexander JS, Peterson ML, Brekken RA, Hirashima M, Capoor S, Usui T, Ambati BK, Ambati J. Alternatively spliced vascular endothelial growth factor receptor-2 is an essential endogenous inhibitor of lymphatic vessel growth. Nat Med. 2009; 15:1023–1030. [PubMed: 19668192]
32. Chen L, Hamrah P, Cursiefen C, Zhang Q, Pytowski B, Streilein JW, Dana MR. Vascular endothelial growth factor receptor-3 mediates induction of corneal alloimmunity. Nat Med. 2004; 10:813–815. [PubMed: 15235599]
33. Han KY, Chang JH, Dugas-Ford J, Alexander JS, Azar DT. Involvement of lysosomal degradation in VEGF-C-induced down-regulation of VEGFR-3. FEBS letters. 2014; 588:4357–4363. [PubMed: 25281926]

Highlights

- Corneal hemangiogenesis and lymphangiogenesis were imaged after corneal injury.
- Only debridement of the entire corneal epithelium induced neovascularization.
- Bulbar conjunctival epithelial debridement did not induce neovascularization.
- More hemangiogenesis than lymphangiogenesis was observed after debridement injury.

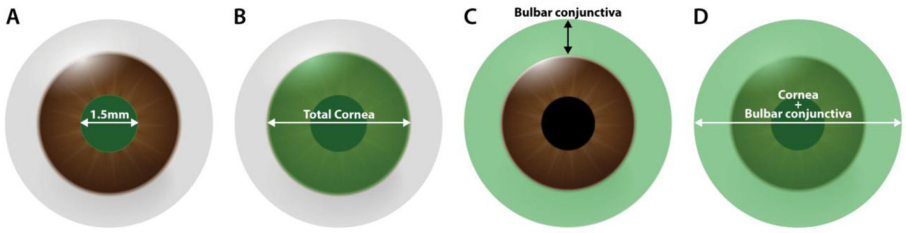

Figure 1.

The four injury models used to perform epithelial debridement of the: (A) central cornea, (B) total cornea, (C) bulbar conjunctiva (excluding the forniceal and palpebral conjunctiva), and (D) cornea+bulbar conjunctiva.

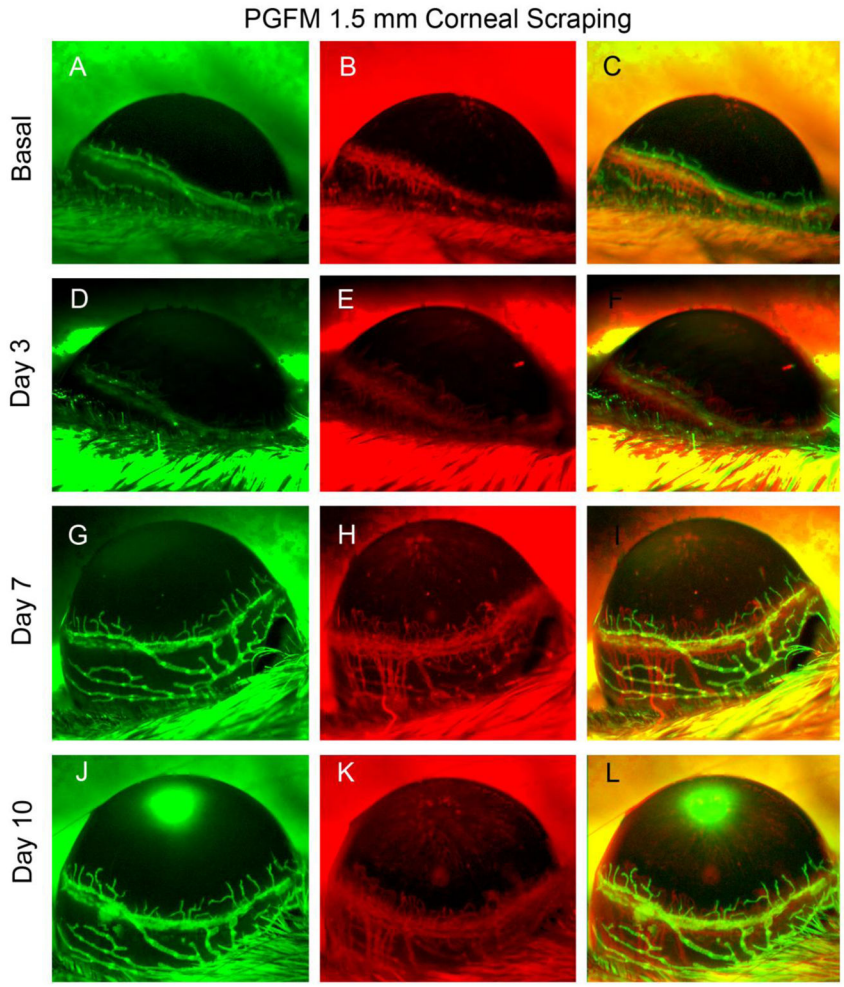

Figure 2.

Central (1.5 mm) corneal debridement. *In vivo* observation of LA and HA in a single *Prox1-GFP/Flk1::myr-mCherry* mouse eye during the 10 days following debridement of the epithelium in the center of the cornea (a 1.5-mm-diameter circle centered at the corneal apex). Representative images were obtained using Axiozoom microscopy of GFP-expressing lymphatic vessels (green, left column) and mCherry-expressing blood vessels (red, right column). The images shown in the figure were acquired at each time point in the same eye.

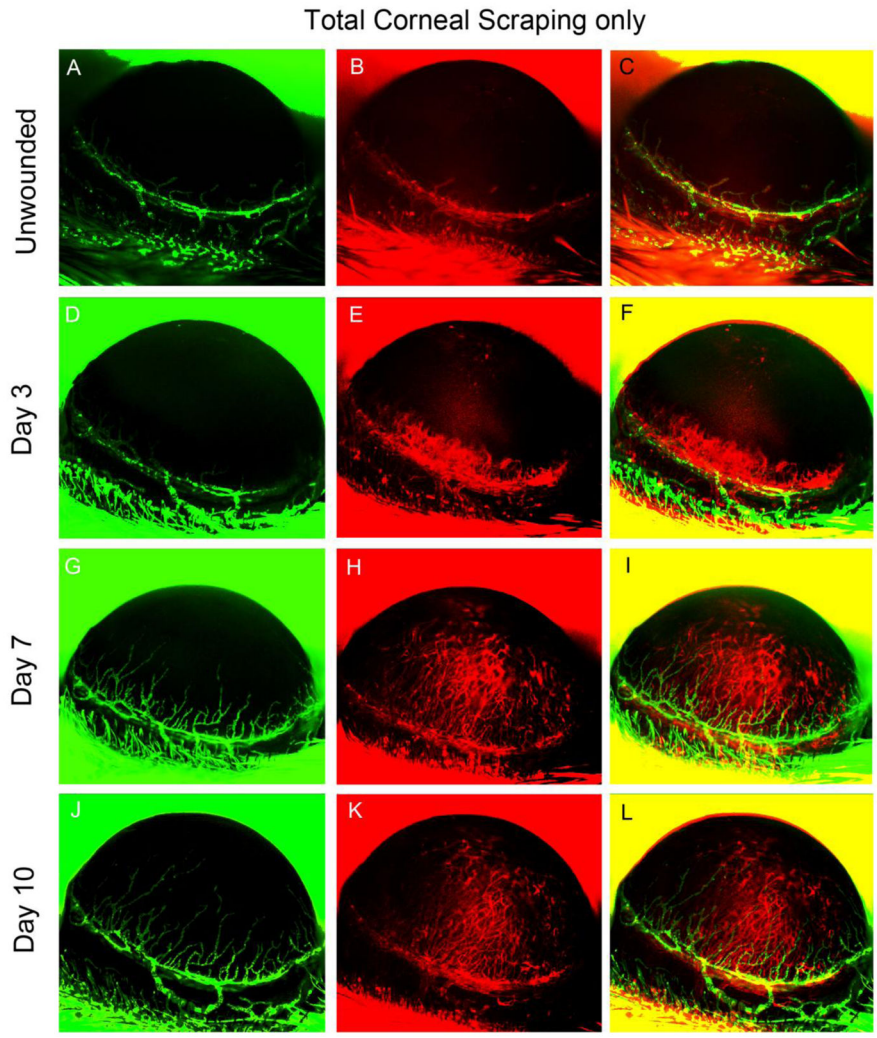

Figure 3.

Total corneal debridement. *In vivo* observation of LA and HA in a single *Prox1-GFP/Flk1::myr-mCherry* mouse eye over 10 days after total corneal epithelial debridement was performed. Representative images were obtained using Axiozoom microscopy of GFP-expressing lymphatic vessels (green, left column) and mCherry-expressing blood vessels (red, right column). The images shown in the figure were acquired at each time point in the same eye.

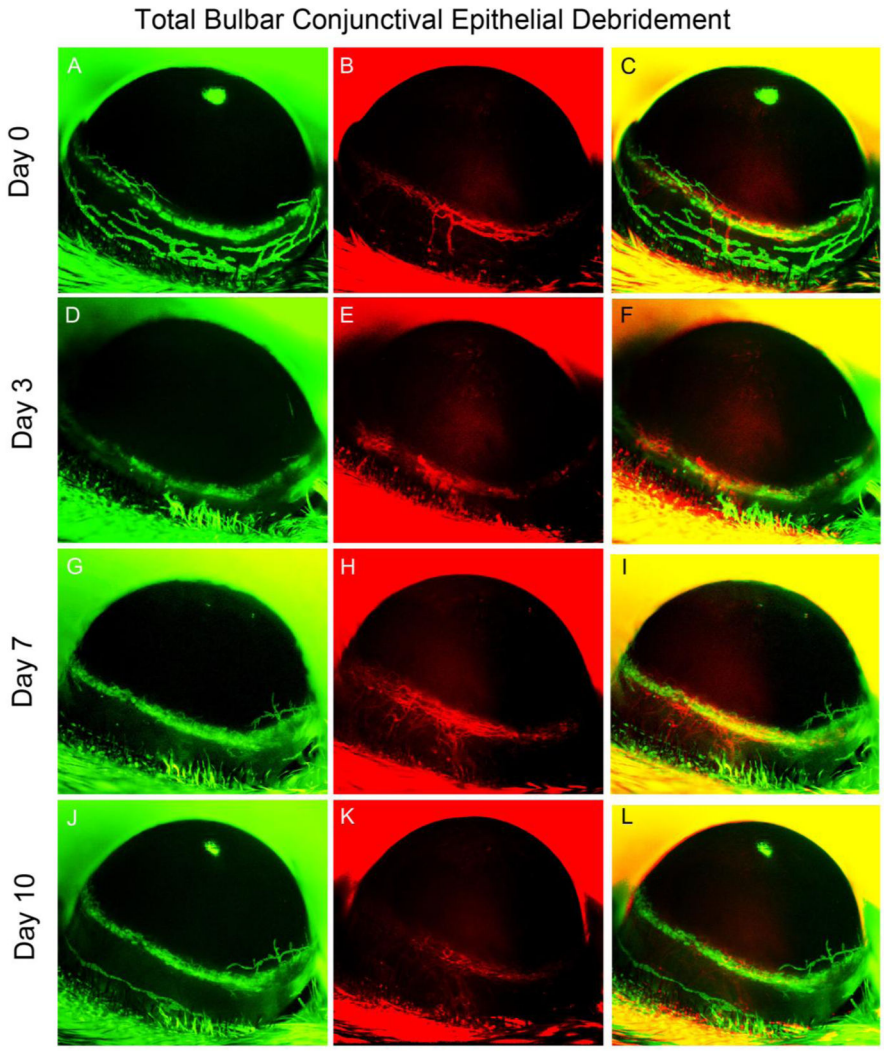

Figure 4.

Bulbar conjunctival debridement. *In vivo* observation of LA and HA in a single *Prox1-GFP/Flk1::myr-mCherry* mouse eye over 10 days after bulbar conjunctival epithelial debridement. Representative images were obtained using Axiozoom microscopy to obtain images of GFP-expressing lymphatic vessels (green, left column) and mCherry-expressing blood vessels (red, right column). The images shown were acquired at each time point in the same eye.

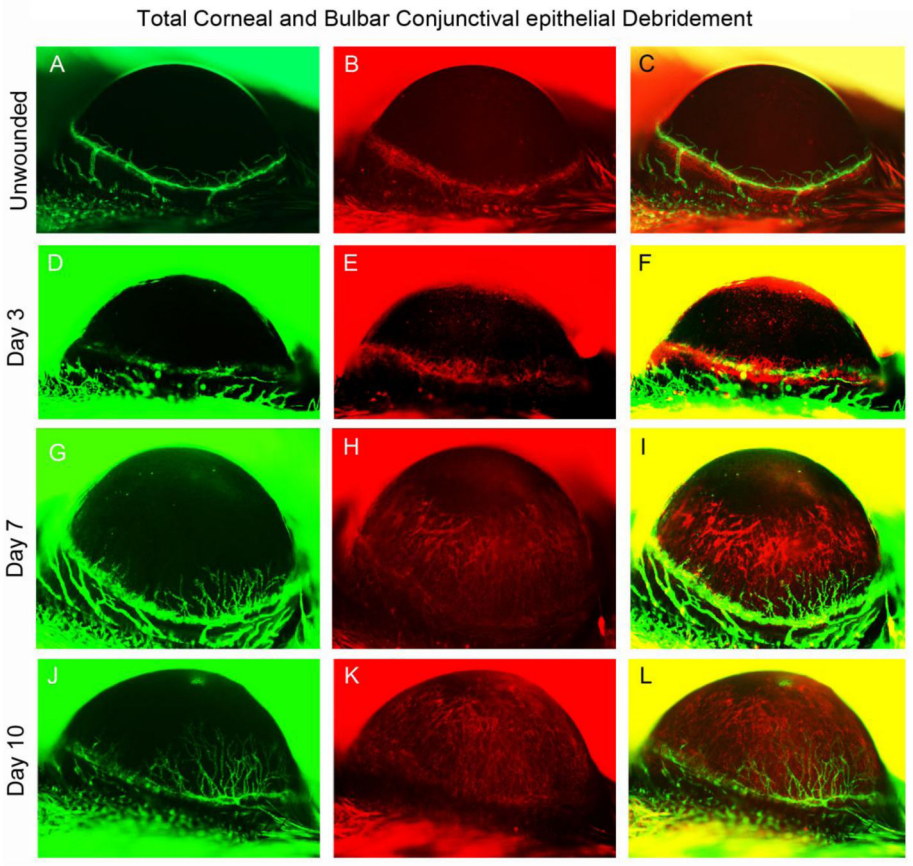

Figure 5.

Total corneal+bulbar conjunctival debridement. *In vivo* observation of LA and HA in a single *Prox1-GFP/Flk1::myr-mCherry* mouse eye during the 10 days following corneal +bulbar conjunctival epithelial debridement. Representative images were obtained using Axiozoom microscopy of GFP-expressing lymphatic vessels (green, left column) and mCherry-expressing blood vessels (red, right column). The images shown were acquired at each time point in the same eye.

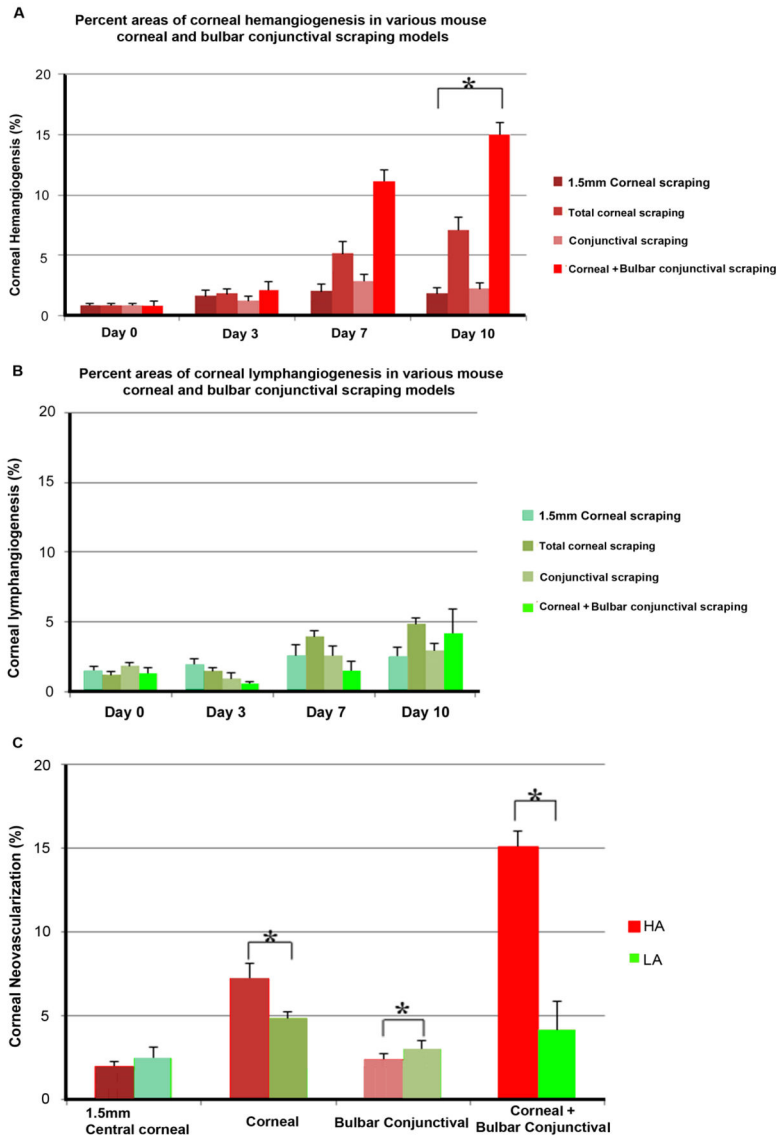

Figure 6.

Quantification of corneal NV after injury by debridement. (A) Percentage of the corneal area that was occupied by HA at the observed time points after injury. (B) Percentage of the corneal area that was occupied by LA at the observed time points after injury. $*P < 0.05$ compared to the untreated group (day 0). (C) Comparison of quantitative data for HA and LA at day 10 in the four treatment groups. $*P < 0.05$ compared to the total corneal debridement group at the same time point.

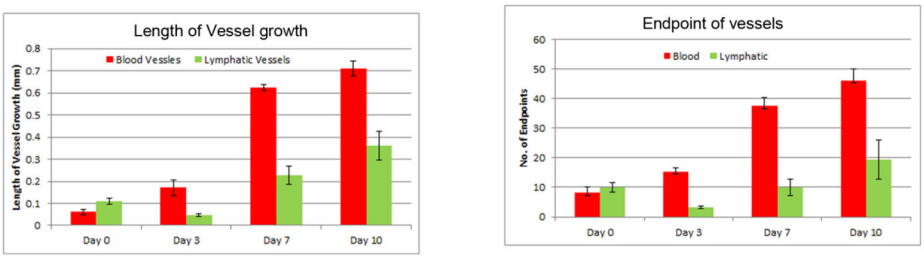

Figure 7.

Comparison of the length of growing vessels and number of endpoints observed in both blood and lymphatic vessels at time points over a period of 10 days in the total corneal + bulbar conjunctival debridement model.

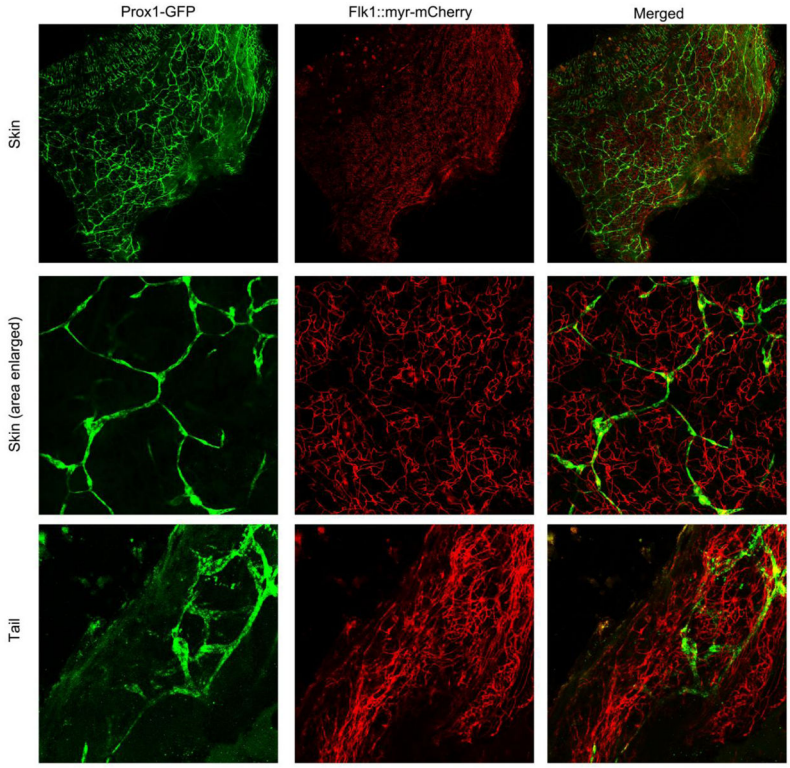

Figure 8.

Confocal microscopy imaging of Prox1-GFP/Flk1::myr-mCherry skin and tail. Mouse skin and tail were harvested and subjected to confocal microscopy imaging.